Natural convection in an inclined porous cavity with variable porosity and thermal dispersion effects

Received February 1996
Revised August 1996

Shih-Wen Hsiao
Department of Industrial Design, National Cheng-Kung University, Tainan, Taiwan, ROC

Nomenclature

A = aspect ratio of the cavity, L_1/L_2
a, b = Ergun constant
B = constant defined in equation (7)
C = coefficient in the dispersion diffusivity
Cp = specific heat at constant pressure
Da = Darcy number, K/L_2^2
Da_∞ = bulk Darcy number
F = Forchheimer coefficient
f = quantity defined in equation (25)
g = gravitational acceleration
k_c = stagnant thermal conductivity
$k_{c\infty}$ = bulk stagnation conductivity
k_d = dispersive thermal conductivity
k_e = effective conductivity of the porous medium
k_f = thermal conductivity of fluid
k_s = thermal conductivity of solid
K = permeability
K_∞ = bulk permeability
L_1 = width of the cavity
L_2 = height of the cavity
l = dispersive length
m = number of iteration
Nu = local Nusselt number
$\overline{Nu}$ = mean Nusselt number
Pr_f = Prandtl number of fluid
Pr_m = media Prandtl number
p^*, p = dimensional and dimensionless pressure
Ra_f = Rayleigh number of fluid, $g\beta_f(T_h^* - T_c^*)L_2^3/\upsilon_f\alpha_f$
Ra_m = media Rayleigh number, $K_{m\infty}\, g\beta f\Delta T^* L_2/\upsilon_f\alpha_m$
T^*, T = dimensional and dimensionless temperature
u^*, u = dimensional and dimensionless Darcian velocities in the x^*–direction
v^*, v = dimensional and dimensionless Darcian velocities in the y^*–direction
$|v^*|, |\bar{v}|$ = dimensional and dimensionless absolute velocities
x^*, x = dimensional and dimensionless horizontal co-ordinates
y^*, y = dimensional and dimensionless vertical co-ordinates

Greek symbols

α_e = effective thermal diffusivity, $k_e/\rho_f Cp_f$
α_f = thermal diffusivity of fluid, $k_f/\rho_f Cp_f$
β_f = thermal expansion coefficient of fluid
Γ = dimensionless particle diameter, dp/L_2
μ_f = dynamic viscosity of fluid
υ_f = kinematic viscosity of fluid
ρ_f = density of fluid
ε = porosity
λ = thermal conductivity ratio of fluid and solid phases
θ = inclined angle of the cavity
Ψ = dimensionless stream function
Ω = dimensionless vorticity
∇^2 = Laplace operator in the (x, y) co-ordinates
η = dimensionless co-ordinate based on particle diameter, x^*/d_p

Introduction

Natural convection within enclosures filled with a porous medium has been studied extensively owing to its widespread engineering applications, including geothermal systems, underground spread of pollutants, storage of nuclear

International Journal for Numerical Methods for Heat & Fluid Flow
Vol. 8 No. 1, 1998, pp. 97–117.

waste materials, solidification of casting, thermal insulation and electronic cooling. Most of the early theoretical studies were based on Darcy's law with the assumption of a uniform porosity medium (Cheng, 1978). It was found that the Nusselt number of the problem depends only on the Rayleigh number and the aspect ratio. However, the experimental results (Seki *et al.*, 1978; Prasad *et al.*, 1985) show that the Nusselt number depends not only on the Rayleigh number and the aspect ratio, but also on the Prandtl number, the Darcy number and the thermal conductivity ratio of the fluid and solid phases.

A number of effects which were neglected in early analyses owing to the limitations of the Darcy's law have recently been investigated. Chan *et al.* (1970), Tong and Subramanian (1985) and Lauriat and Prasad (1986) have studied the viscous effects using the Brinkman-extended Darcy equations. Tong and Subramanian (1985) found that pure Darcy analysis is applicable only when $RaDa^2/A < O(10^{-4})$. The inertia effects have been investigated by Poulikakos (1985) who used the Forchheimer-extended Darcy model. Beckermann *et al.* (1986) have studied the inertia and viscous effects using the Brinkman-Forchheimer-extended Darcy equations (BFD model), and found that at high Darcy numbers ($Da > 10^{-4}$) the inertia and viscous effects have the same order of magnitude and must be taken into account simultaneously.

The effects of variable porosity on forced convection in porous media have been reported by Vafai (1984), Cheng and Hsu (1986b) and Poulikakos and Renken (1987). It was shown that the porosity variation has important effects on heat transfer if the dimensionless particle diameter is high.

Thermal dispersion effect on natural and mixed convection in a uniform porosity medium of infinite extent was studied by Cheng (1981) and Cheng and Zhang (1986). Thermal dispersion effect on natural and mixed convection in a uniform porosity rectangular cavity heated from below was studied by Georgiadis and Catton (1988). Hong *et al.* (1987a, 1987b) have studied the variable porosity and thermal dispersion effects on natural convection near a vertical plate.

More recently, the effects of particle diameter, Prandtl number, aspect ratio of the cavity, thermal conductivity ratio and bulk porosity on natural convection in a rectangular porous cavity heated from the vertical side wall have been investigated by Davis *et al.* (1988). The variable porosity and thermal dispersion effects on natural convection about a heated horizontal cylinder in an enclosed porous medium was studied by Hsiao *et al.* (1992).

Though effects of individual parameter have been investigated in the previously mentioned works, they are almost focused on effects of individual parameter or few parameters only. To the author's knowledge, no investigations aimed at integrating parameters of affecting the flow and heat transfer characteristics of natural convection in a porous cavity together to study the coupling effects between different parameters and to suggest a better model for simulating a porous cavity have been proposed. To achieve this objective, a more complete model is adopted in this study in which the effects of variable

porosity, thermal dispersion, conductivity ratio of the fluid and solid phases, Prandtl number, dimensionless particle diameter, and inclined angle of the cavity on natural convection in a porous cavity are all considered. In this model, the coupling effects due to different parameters can be investigated. The non-Darcian effects are included in the momentum equation, and the thermal dispersion effect is considered in the energy equation. The wall effect on porosity is approximated by an exponential function (Cheng, 1986) and its effect on thermal dispersion is modeled by the dispersive length concept proposed by Cheng and Hsu (1986a) and Hsu and Cheng (1988). The governing equations in terms of stream function, vorticity and temperature are solved by the finite difference method. The streamlines, isotherms, temperature and velocity distributions, and average Nusselt numbers at different Rayleigh numbers, Prandtl numbers, dimensionless particle diameters and inclined angles are presented. It is found that the variable porosity and thermal dispersion effects tend to increase the heat transfer rate. The effect of the thermal conductivity of the solid phase on the Nusselt number is greater at low Rayleigh numbers where conduction heat transfer is predominant. The predicted Nusselt numbers which take into account the effects of non-Darcian, variable porosity and thermal dispersion have the best agreement with existing experimental data.

Mathematical formulation

A schematic of the physical model and co-ordinate system is shown in Figure 1. Two opposite isothermal walls of the inclined rectangular cavity were kept at different temperatures while the other walls were thermally insulated.

The governing equations for the conservation of mass, momentum and energy in Cartesian co-ordinates for the problem of steady natural convection in a variable porosity medium according to the Boussinesq approximation are:

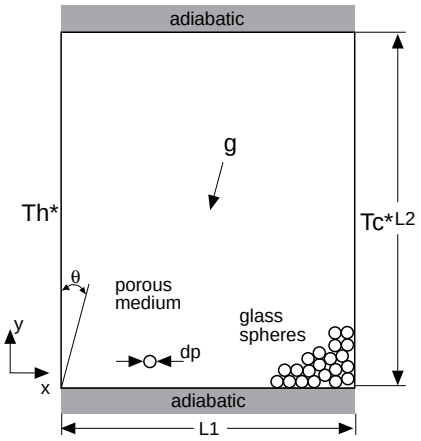

Figure 1.
Physical model and co-ordinate system

$$\nabla \cdot \bar{v}^* = 0$$

$$\rho_f \nabla \cdot \left(\frac{\bar{v}^* \cdot \bar{v}^*}{\epsilon} \right) = -\nabla p^* + \mu_f \nabla^2 \bar{v}^* - \frac{\mu_f \epsilon \bar{v}^*}{K} \tag{1}$$

$$- \frac{\rho_f F |\bar{v}^*| \bar{v}^* \epsilon}{\sqrt{K}} + \rho_f \beta_f (T^* - T_c^*) \epsilon g \tag{2}$$

$$(\rho Cp)_f \bar{v}^* \cdot \nabla T^* = \nabla \cdot (k_e \nabla T^*) \ , \tag{3}$$

where $\bar{v}^*$ and $\bar{p}^*$ are the volume-averaged velocity vector and pressure. K and F are the permeability and the inertial coefficient of the porous medium which are given by the following correlations for a packed-sphere bed:

$$K = \frac{\epsilon^3 \, dp^2}{a(1-\epsilon)^2} \tag{4}$$

$$F = \frac{b}{\sqrt{a} \ \epsilon^{3/2}} \ . \tag{5}$$

Here, a and b are empirical constants, dp is the particle diameter, and ϵ is the porosity which is assumed to vary exponentially with distance from the walls (Chandrasekhara and Vortmeyer, 1979) such that:

$$\epsilon = \epsilon_\infty + (\epsilon_\circ - \epsilon_\infty) \exp(-N_1 x^*/dp) \ , \tag{6}$$

where x^* is the distance from the wall, N_1 is an empirical constant, and ϵ_∞ and ϵ_0 are the porosities at locations far away and on the wall, respectively.

The quantity k_e in equation (3) is the effective thermal conductivity of the saturated porous medium which is a superposition of the stagnant thermal conductivity (k_c) and the dispersive conductivity (k_d); i.e. $k_e = k_c + k_d$.

The value of the stagnant thermal conductivity of the saturated porous medium can be computed according to the semi-analytical expression given by Zehner *et al.* (1970) as

$$\frac{k_c}{k_f} = (1 - \sqrt{1 - \epsilon}) + \frac{2\sqrt{1-\epsilon}}{1 - \lambda B} \left[\frac{(1 - \lambda)}{(1 - \lambda} \right.$$

$$\left. - \frac{B + 1}{2} - \frac{B - 1}{1 - \lambda B} \right] , \tag{7}$$

where $B = 1.25[(1 - \epsilon)/\epsilon]^{10/9}$ and $\lambda = k_f/k_s$ where k_f and k_s denote the thermal conductivity of the fluid and the solid phases respectively.

The value of k_s for a glass bead is calculated based on the expression (Fand and Phan, 1987)

$$k_s = 1.00416 + 1.6736\times10^{-3}T^* - 4.184\times10^{-6}T^{*2}, \tag{8}$$

where T^* is the temperature in centigrade and k_s is expressed in w/m°C.

The thermal dispersion conductivity for flow through a porous medium is given by Cheng and Hsu (1986a) and Hsu and Cheng (1988).

$$k_d = C(\rho Cp)_f|\bar{v}^*|l\,dp\,. \tag{9}$$

Here l is the dispersive length which is given by

$$l = \frac{1-\epsilon}{\epsilon}, \tag{10}$$

while $|\bar{v}^*| = (u^{*2} + v^{*2})^{1/2}$ and the dispersivity value, $C = 0.02$, was determined by a comparison of theoretical and experimental results (Hsu and Cheng, 1988). We now introduce the following dimensionless variables:

$$x = \frac{x^*}{L_2},\quad y = \frac{y^*}{L_2},\quad u = \frac{u^*L_2}{\alpha_f},\quad v = \frac{v^*L_2}{\alpha_f},$$

$$T = \frac{T^* - T_c^*}{T_h^* - T_c^*},\quad p = \frac{p^*L_2}{\rho_f\alpha_f^2}\,. \tag{11}$$

In terms of these variables, the governing equations become

$$\frac{\partial u}{\partial x} + \frac{\partial v}{\partial y} = 0 \tag{12}$$

$$u\frac{\partial}{\partial x}\left(\frac{u}{\epsilon}\right) + v\frac{\partial}{\partial y}\left(\frac{u}{\epsilon}\right) = -\frac{\partial p}{\partial x} + Pr_f\nabla^2 u - \left(\frac{Pr_f}{Da} + \frac{F}{\sqrt{Da}}|\bar{v}|\right)\epsilon u + Ra_f Pr_f \epsilon T\sin\theta \tag{13}$$

$$u\frac{\partial}{\partial x}\left(\frac{v}{\epsilon}\right) + v\frac{\partial}{\partial y}\left(\frac{v}{\epsilon}\right) = -\frac{\partial p}{\partial y} + Pr_f\nabla^2 v$$

$$-\left(\frac{Pr_f}{Da}+\frac{F}{\sqrt{Da}}|\bar{v}|\right)\epsilon v + Ra_f Pr_f \epsilon T\cos\theta \tag{14}$$

$$u\frac{\partial T}{\partial x}+v\frac{\partial T}{\partial y}=\frac{\partial}{\partial x}\left(\frac{\alpha_e}{\alpha_f}\frac{\partial T}{\partial x}\right)+\frac{\partial}{\partial y}\left(\frac{\alpha_e}{\alpha_f}\frac{\partial T}{\partial y}\right), \tag{15}$$

where α_e, Pr_f, and Ra_f are the effective thermal diffusivity of the saturated porous medium, the Prandtl number, and the Rayleigh number respectively, which are defined as

$$\alpha_e=\frac{k_e}{(\rho\ Cp)_f}, \qquad Pr_f=\frac{\nu_f}{\alpha_f},$$

$$Ra_f=\frac{g\beta_f(T_h^*-T_c^*)L_2^3}{\alpha_f\ \nu_f}. \tag{16}$$

Da is the local Darcy number which is defined as

$$Da=\frac{K}{L_2^2}. \tag{17}$$

The local Darcy number is related to the bulk Darcy number (Da_∞) by

$$Da=Da_\infty\frac{K}{K_\infty}=Da_\infty\left(\frac{\epsilon}{\epsilon_\infty}\right)^3\left(\frac{1-\epsilon_\infty}{1-\epsilon}\right)^2, \tag{18}$$

where

$$Da_\infty=K_\infty/L_2^2=\frac{\Gamma^2\ \epsilon_\infty^{\ 3}}{a(1-\epsilon_\infty)^2} \quad \text{with } K_\infty$$

denoting the bulk permeability and $\Gamma = dp/L_2$.

Eliminating the pressure terms in equations (13) and (14), the resulting nondimensional equations for the stream function, vorticity, and temperature are given by

$$\nabla^2\Psi = -\Omega \tag{19}$$

$$\frac{\partial}{\partial x}\left[\frac{\partial\Psi}{\partial y}\frac{\partial}{\partial x}\left(\frac{-1}{\epsilon}\frac{\partial\Psi}{\partial x}\right) - \frac{\partial\Psi}{\partial x}\frac{\partial}{\partial y}\left(\frac{-1}{\epsilon}\frac{\partial\Psi}{\partial x}\right)\right]$$

$$-\frac{\partial}{\partial y}\left[\frac{\partial\Psi}{\partial y}\frac{\partial}{\partial x}\left(\frac{1}{\epsilon}\frac{\partial\Psi}{\partial y}\right) - \frac{\partial\Psi}{\partial x}\frac{\partial}{\partial y}\left(\frac{1}{\epsilon}\frac{\partial\Psi}{\partial y}\right)\right]$$

$$= \mathrm{Pr}_f\nabla^2\Omega - \left[\left(\frac{\mathrm{Pr}_f}{\mathrm{Da}} + \frac{F}{\sqrt{\mathrm{Da}}}|\bar{v}|\right)\epsilon\right]\Omega + \frac{\partial\Psi}{\partial y}\frac{\partial}{\partial y}\left[\left(\frac{\mathrm{Pr}_f}{\mathrm{Da}} +\right.\right.$$

$$+ \mathrm{Ra}_f\mathrm{Pr}_f\left[\frac{\partial}{\partial x}(\epsilon T)\cos\theta - \frac{\partial}{\partial y}(\epsilon T)\sin\theta\right] \tag{20}$$

$$\frac{\partial\Psi}{\partial y}\frac{\partial T}{\partial x} - \frac{\partial\Psi}{\partial x}\frac{\partial T}{\partial y} = \frac{\partial}{\partial x}\left(\frac{\alpha_e}{\alpha_f}\frac{\partial T}{\partial x}\right)$$

$$+ \frac{\partial}{\partial y}\left(\frac{\alpha_e}{\alpha_f}\frac{\partial T}{\partial y}\right) , \tag{21}$$

where the dimensionless stream function and vorticity are defined as

$$u = \frac{\partial\Psi}{\partial y}, \quad v = -\frac{\partial\Psi}{\partial x}, \quad \Omega = \frac{\partial v}{\partial x} - \frac{\partial u}{\partial y} . \tag{22}$$

In terms of the dimensionless co-ordinates, equation (6) becomes

$$\epsilon = \epsilon_\infty + (\epsilon_o - \epsilon_\infty)\exp(-N_1 x/\Gamma) , \tag{23}$$

where $\Gamma = dp/L_2$ is the dimensionless particle diameter.

The dimensionless boundary conditions are:

$$\frac{\partial\Psi}{\partial x} = \Psi = 0, \; T = 1, \; \Omega = -\Psi_{xx} \quad \text{at } x = 0, \; 0 \le y \le 1 \tag{24a}$$

$$\frac{\partial\Psi}{\partial x} = \Psi = 0, \; T = 0, \; \Omega = -\Psi_{xx} \quad \text{at } x = \frac{L_1}{L_2}, \; 0 \le y \le 1 \tag{24b}$$

$$\frac{\partial\Psi}{\partial y} = \Psi = 0, \; \frac{\partial T}{\partial y} = 0, \; \Omega = -\Psi_{yy} \quad \text{at } 0 \le x \le \frac{L_1}{L_2}, \; y = 0 \tag{24c}$$

$$\frac{\partial \Psi}{\partial y} = \Psi = 0, \frac{\partial T}{\partial y} = 0, \Omega = -\Psi_{yy} \text{ at } 0 \leq x \leq \frac{L_1}{L_2}, \; y = 1 \quad (24d)$$

Numerical procedures

The governing equations, (19)-(21), are discretized by the finite difference method based on second order differencing, and the resulting finite difference equations are solved by the successive over-relaxation (SOR) technique. The necessary number of grid points depends on the Rayleigh number, the aspect ratio of the cavity ($A = L_1/L_2$), and the particle diameter. Trial calculations were necessary to check computation accuracy. The grid space near the wall should be less than one-third of the particle diameter if accurate results are to be obtained. It was found that a uniform grid of 101×101 is needed for a square cavity to obtain accurate temperature and velocity gradients near the wall and Nusselt number as well for the cases of considering the variable porosity and thermal dispersion effects. If smaller grid umbers are needed, a nonuniform grid is suggested, but the density of grids near the wall should be controlled. However, a grid of 61×61 is required only to obtain accurate results for cases with constant porosity and neglecting thermal dispersion effect.

The numerical solutions were obtained using an iterative process which was repeated until the following convergence criterion was satisfied:

$$\left| \frac{f^{m+1} - f^{m}}{f^{m+1}} \right| \leq 10^{-4} . \quad (25)$$

Here f is a general symbol used for Ψ, Ω, and T and m is the iteration number. Computations were also carried out for the local and mean Nusselt numbers along the hot wall, which are defined as follows:

$$Nu = \frac{h \, L_2}{k_f} = -\frac{\partial T}{\partial x}\Big|_{x=0} \quad (26)$$

$$\overline{Nu} = \frac{1}{L_2} \int_0^{L_2} Nu \, dy \; . \quad (27)$$

Results and discussion

The parameters shown in the governing equations and boundary conditions are particle diameter, Prandtl number, aspect ratio of the cavity, thermal conductivity ratio of fluid and solid phases, porosity and inclined angle of the cavity. In equations (4)-(6), some empirical constants should be used to estimate the permeability and porosity of a packed-sphere bed. The combination of empirical constants $\epsilon_\omega = 0.36$, $\epsilon_0 = 0.9$, $N_1 = 7$, $a = 215$, and $b = 1.92$ proved to be best for obtaining results in good agreement with experimental data by

Hsiao *et al.* (1992). Thus, the numerical results presented in this paper were obtained using these constants.

Accuracy of the numerical solutions

The accuracy of the numerical algorithm was checked by comparing the present results for the Nusselt number with values reported in literature.

In Table I, previous numerical results in Nusselt numbers are compared with present predictions for cases with constant porosity and neglecting thermal dispersion. In this table, the parameter Pr_m represents the modified Prandtl number which is defined as $Pr_m = \upsilon_f/\alpha_e$. Weber (1975) obtained results using the pure Darcy model. The values of Tong and Subramanian (1985) were obtained based on the Brinkman-Darcy model with a boundary layer approximation, and those of Beckermann *et al.*(1986) were obtained using the Brinkman-Forchheimer-Darcy model. It is found that the present Nusselt numbers for constant porosity medium ($\alpha_e/\alpha_f = 1.4$) are in good agreement with those of Beckermann *et al.* (1986) . This is due to the fact that the constant porosity model in this work is the same as that of Beckermann's. By comparing with the results of Beckermann *et al.* (1986), the accuracy of this work is assured.

Cases	Ra_f	Da	A	Pr_m	Weber (25)	Tong (5)	Beckermann (8)	Present results
Heated	1.598×10^9	8.125×10^{-7}	2.25	4	13.9	13.5	11.15	11.23
from	1.997×10^9	8.125×10^{-7}	2.25	4	15.5	15.0	12.61	12.70
below	9.969×10^7	3.250×10^{-6}	2.25	4	4.9	4.8	4.54	4.61
$\theta = 90°$	1.994×10^8	3.250×10^{-6}	2.25	4	6.9	6.8	6.62	6.71

Table I. Comparison of Nusselt numbers from present and previous numerical models for a uniform porous medium

Effect of Prandtl number

The effects of Prandtl number on the mean Nusselt numbers for porous cavities with uniform porosity (dashed line) and variable porosity (solid line) are presented in Figures 2 and 3. Figure 2 shows Prandtl number effects of the fluid on the average Nusselt number for a square porous cavity with $\lambda = 0.6$, and $\Gamma = 0.04$ and 0.2. It is shown that the Nusselt number increases with the Prandtl number. If the Prandtl number is greater than one, its effects on the Nusselt number are small for both uniform and variable porosity media. The Prandtl number effect on the Nusselt number increases if the Prandtl number is less than one, which is in agreement with experimental observations (Jonsson and Catton, 1987) . Figure 3 shows the Prandtl number effect on the average Nusselt number as a function of Rayleigh number for natural convection in a square cavity heated from below ($\theta = 90°$) with $\lambda = 0.6$ and $\Gamma = 0.2$. It is clear that Prandtl number effects on the average Nusselt number are small for $Pr > 1$.

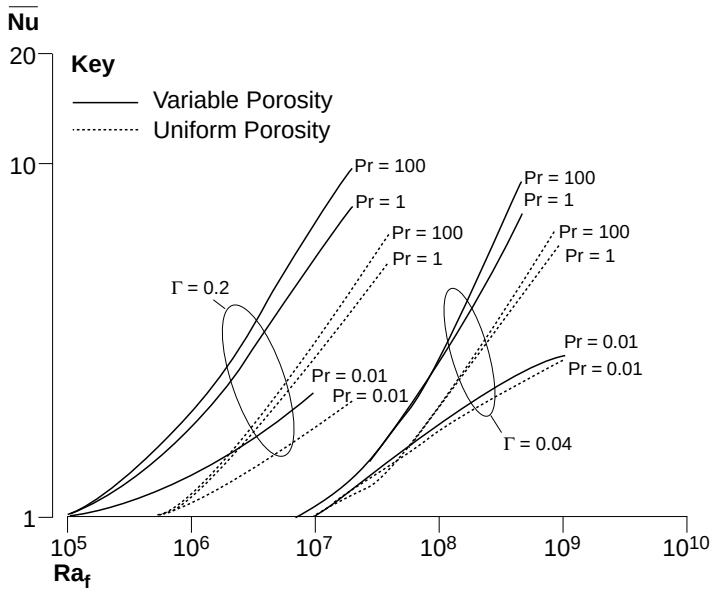

Figure 2.
Effect of Prandtl number and dimensionless particle diameter on Nusselt number for a square porous cavity heated from the side

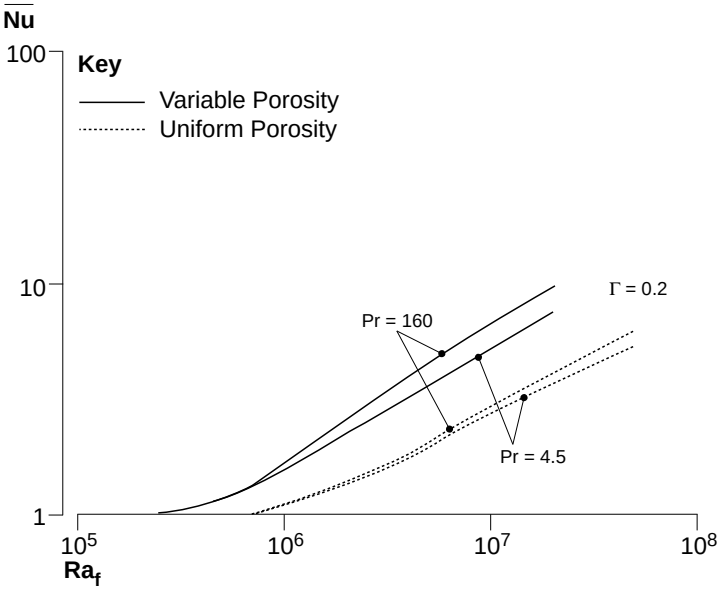

Figure 3.
Effect of Prandtl number on mean Nusselt number for a square porous cavity heated from below ($\theta = 90°$)

Effect of dimensionless particle diameter

Figure 4 depicts the effects of dimensionless particle diameter on the mean Nusselt number for a porous cavity heated from below ($\theta = 90°$) with $A = 1$ and $\lambda = 0.6$, where the dashed lines represent the results for a uniform porosity medium and the solid lines represent those for a variable porosity medium. The

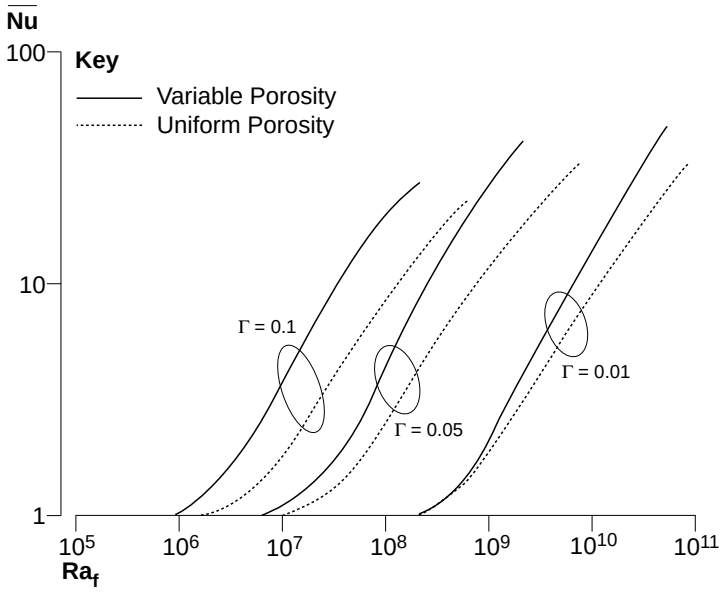

Figure 4.
Effect of dimensionless particle diameter on the mean Nusselt number for a square porous cavity ($\theta = 90°$)

effect of variable porosity on Nusselt number increases with the dimensionless particle diameter. Because the porosity of the medium increases with the diameter of the particle, and the porosity effect increases the temperature gradient adjacent to the wall, this results in the enhancement of surface heat flux.

It is also found that the value of the Rayleigh number for the onset of free convection is reduced as dimensionless particle diameter is increased. Comparing the solid curves, we see that, in a variable porosity medium, the slopes of the curves start to decrease at lower Rayleigh numbers as the value of Γ is increased, which is similar to the results obtained by heating from the vertical side wall (Davis *et al.*, 1988).

Effect of thermal conductivity ratio

The effects of the thermal conductivity ratio of the fluid and solid phases on the mean Nusselt number of a square cavity filled with a uniform porosity medium and a variable porosity medium with $Pr_f = 5$, $A = 1$, and $\Gamma = 0.1$ are shown in Figures 5 and 6. Figure 5 shows the effects of the thermal conductivity ratio on the average Nusselt number for a porous cavity heated from the side ($\theta = 0°$). The dashed lines represent the results for a uniform porosity medium while the solid lines are for a variable porosity medium. For $\lambda = 0.1$ (where the thermal conductivity of the fluid is much smaller than that of the solid) both the solid and dashed lines are horizontal at small Rayleigh numbers indicating that heat conduction is predominant; onset of convection occurs at a larger Rayleigh number (where the lines curve upward). When $\lambda = 10$, however, both the solid and dashed lines curve upward continuously, indicating that convection begins

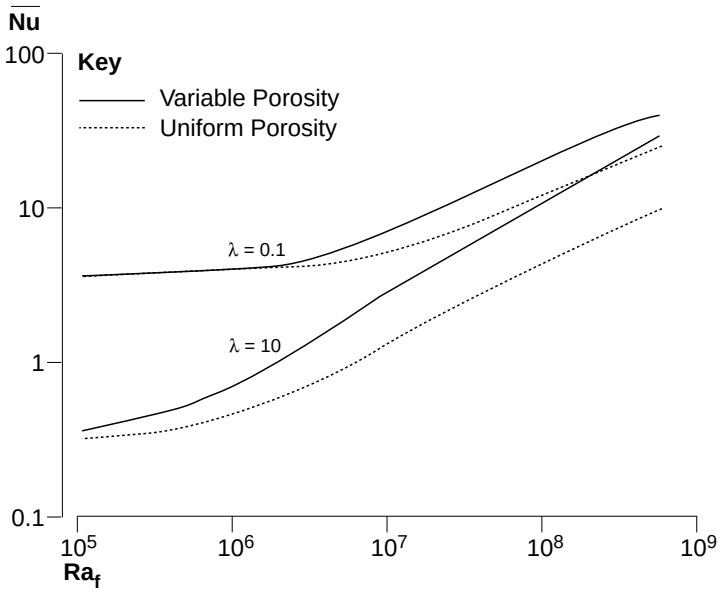

Figure 5.
Effect of thermal conductivity on mean Nusselt number (A = 1, Γ = 0.1, θ = 0°)

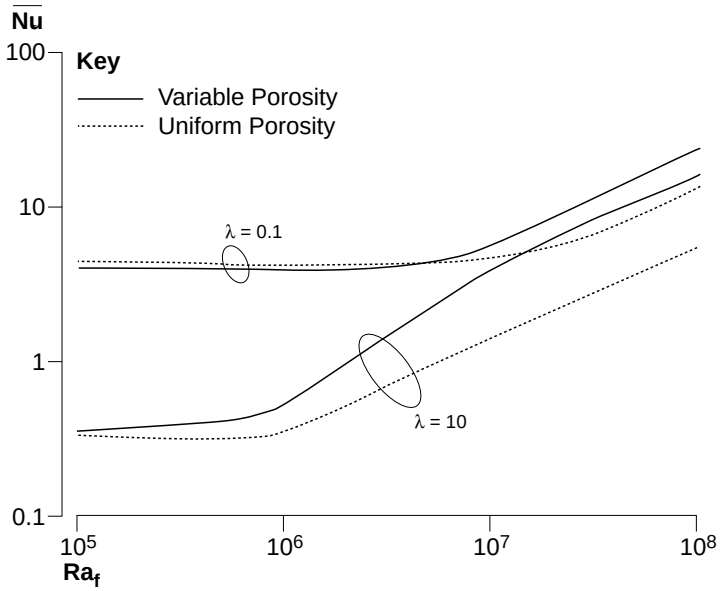

Figure 6.
Effect of thermal conductivity on mean Nusselt number (A = 1, Γ = 0.1, θ = 0°)

at a very small Rayleigh number. Figure 6 shows the effect of thermal conductivity ratio on the average Nusselt number in a square porous cavity heated from below (θ = 90°). It is apparent that the critical Rayleigh number for the onset of free convection decreases as the thermal conductivity ratio increases, as discussed earlier.

Effect of inclination angle of the cavity

The effect of the inclination angle of the cavity (θ) on flow and heat transfer characteristics in a square cavity with uniform porosity at $Ra_f = 10^8$, $\lambda = 0.6$ and $\Gamma = 0.1$ are presented in Figures 7-9. Figure 7 shows the streamlines (right, ($\Delta \Psi = 2$) and isotherms (left, $\Delta T = 0.1$) in a porous cavity with glass beads saturated with water and with the cavity at different inclination angles. It can be seen from these figures that the flow patterns and isotherms varied with the inclination angle. The density of streamlines increases from $\theta = 0°$ to 45°, then decreases from $\theta = 45°$ to 90°, indicating that there is a critical value of θ for which the heat transfer rate is maximum. As the inclination angle is increased to 75°, the flow pattern is still in one convective cell. With further increases in the inclination angle to $\theta = 90°$ as shown in Figure 7(f), the flow pattern becomes two convective cells. It is apparent that the isotherms and streamlines are symmetric about the vertical axis of the cavity, which is consistent with the physical meaning of the problem when the cavity is heated from below. Figure 8 shows the temperature distributions on the symmetric axis perpendicular to the isothermal walls for $\theta = 0°$, 45°, and 90°. It is shown that the distortion of the temperature curve at $\theta = 45°$ is more obvious than those at $\theta = 0°$, and 90°. This result shows that the maximum value of the temperature gradient near the wall occurs at $\theta = 45°$, suggesting that the convective effect is enhanced here.

The effect of the inclination angle on the mean Nusselt number for a rectangular cavity filled with water and glass beads with $A = 1$, $\Gamma = 0.1$, $\lambda = 0.6$, and $Ra_f = 10^8$ is shown in Figure 9. The mean Nusselt number increases with inclination angle from 0° to about 36° and then decreases monotonically to 90°, indicating that the maximum average Nusselt number is located at $\theta = 36°$. These results are in agreement with the experimental data of Inaba *et al.* (1988) which were obtained using water-glass spheres with an aspect ratio $A = 5$.

Effect of variable porosity

Figure 10(a) shows the velocity distribution of the fluid along the horizontal axis of the cavity with $Ra_f = 10^7$, $\Gamma = 0.1$, $A = 1$, $\lambda = 0.6$, and $\theta = 0$ (heated from the side). Figure 10(b) shows the velocity distribution in another case with the same parameters as those in Figure 10(a) except the value of Γ is reduced to 0.01. The results show that the variable porosity creates a channeling effect such that the fluid velocity near the wall is increased, resulting in enhancement of the convection effect. These figures also show that the velocity distribution of the model VPWD (variable porosity with dispersion effect) coincides with that of the model VPND (variable porosity without dispersion effect), and those of the models CPWD (uniform porosity with dispersion effect) and CPND (uniform porosity without dispersion effect) are also consistent. This indicates that the location of the peak velocity is only affected by the particle diameter, not by the variable porosity or the thermal dispersion. These results show that the maximum velocity occurs at about one-third of the particle diameter away from the wall; its magnitude increases as the value of Γ is decreased. Figure 11(a) shows the temperature distribution along the horizontal axis of a cavity with

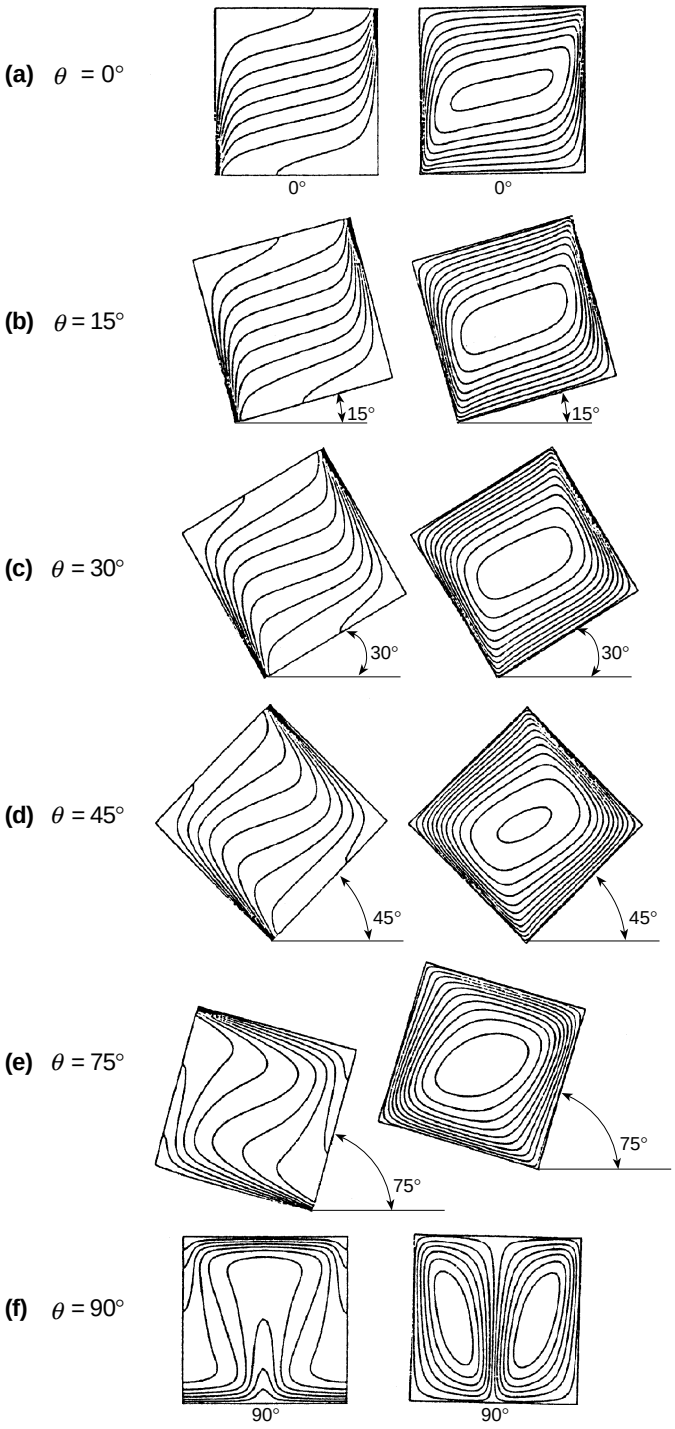

Figure 7.
Steady state streamlines (right, $\Delta\Psi = 2$) and isotherms (left, $\Delta T = 0.1$) in a uniform porosity cavity ($A = 1$, $\Gamma = 0.1$, $Ra_f = 10^8$)

$Ra_f = 10^7$, $\Gamma = 0.05$, $A = 1$, $\lambda = 0.6$ and $\theta = 0°$ (heated from the side), where η in the abscissa represents the dimensionless co-ordinate based on the particle diameter ($\eta = x^*/d_p$). The corresponding velocity distribution is shown in Figure 11(b). It is shown that the curvature of the temperature curve for a variable porosity medium (solid line) is greater than that of a uniform porosity medium (dashed line) in the region near the wall ($\eta < 1.2$), suggesting that the variable porosity effect tends to increase the temperature gradient adjacent to the wall, which results in the enhancement of surface heat flux. The curvature of the temperature curve for a variable porosity medium is less than that for a

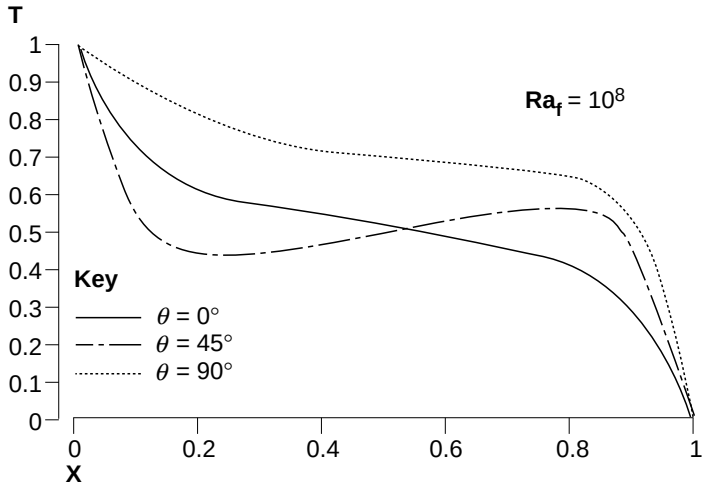

Figure 8.
Temperature profiles on the symmetric axis perpendicular to the isothermal walls of a uniform porosity cavity with $A = 1$, $\Gamma = 0.1$, $\lambda = 0.6$, and $Ra_f = 10^8$ for $\theta = 0°$, 45° and 90°

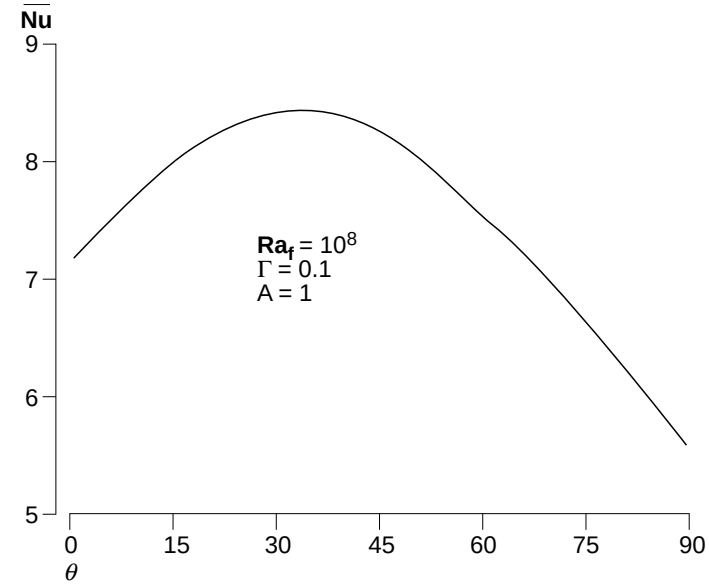

Figure 9.
Effect of inclination angle of the cavity on the mean Nusselt number of a uniform porous cavity $A = 1$, $\Gamma = 0.1$, $\lambda = 0.1$, $Ra_f = 10^8$

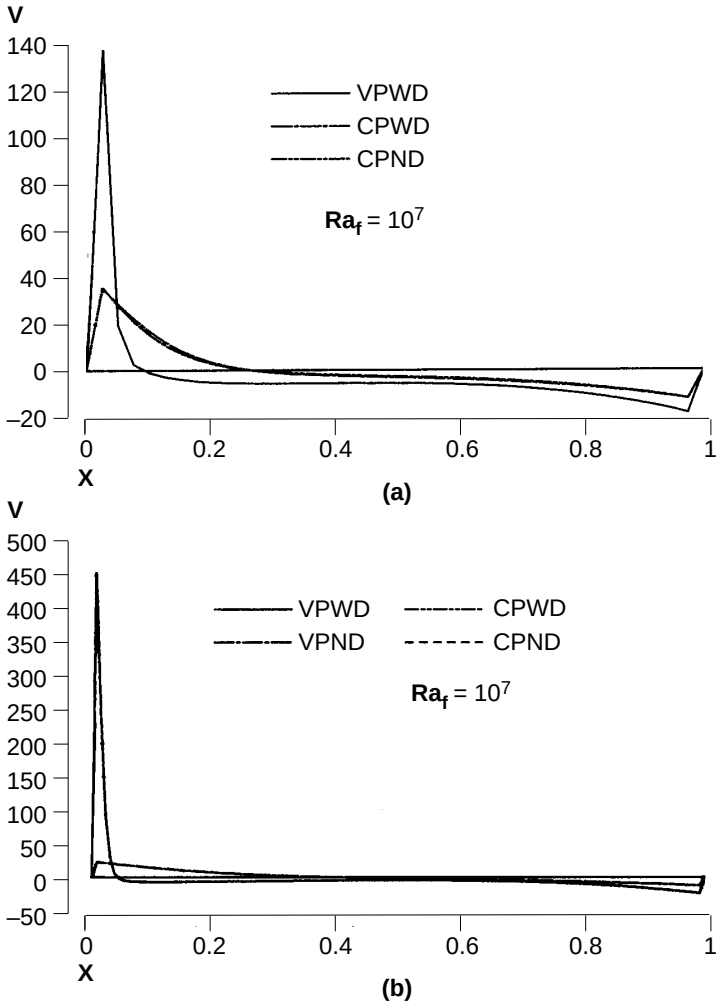

Figure 10.
Velocity distributions for different particle diameters: (a) $A = 1$, $\Gamma = 0.1$, $\theta = 0°$, and $\lambda = 0.6$; (b) $A = 1$, $\Gamma = 0.01$; $\theta = 0°$, and $\lambda = 0.6$

uniform porosity medium in the region of $\eta > 1.2$, which means that the temperature of the variable porosity medium is greater than that of the uniform porosity medium in this region. This is because the variable porosity effect enhanced the surface heat flux such that the heat energy was dispersed far away from the wall.

The effect of variable porosity on the average heat transfer rate is shown in Figures 2-6. The results show that the effect of variable porosity tends to increase the mean Nusselt number in the convection dominated region while it can be neglected in the region dominated by conduction.

Effect of thermal dispersion

The thermal dispersion effect on the mean Nusselt number as a function of dimensionless particle diameter for the water/glass beads system at $Ra_f = 10^8$,

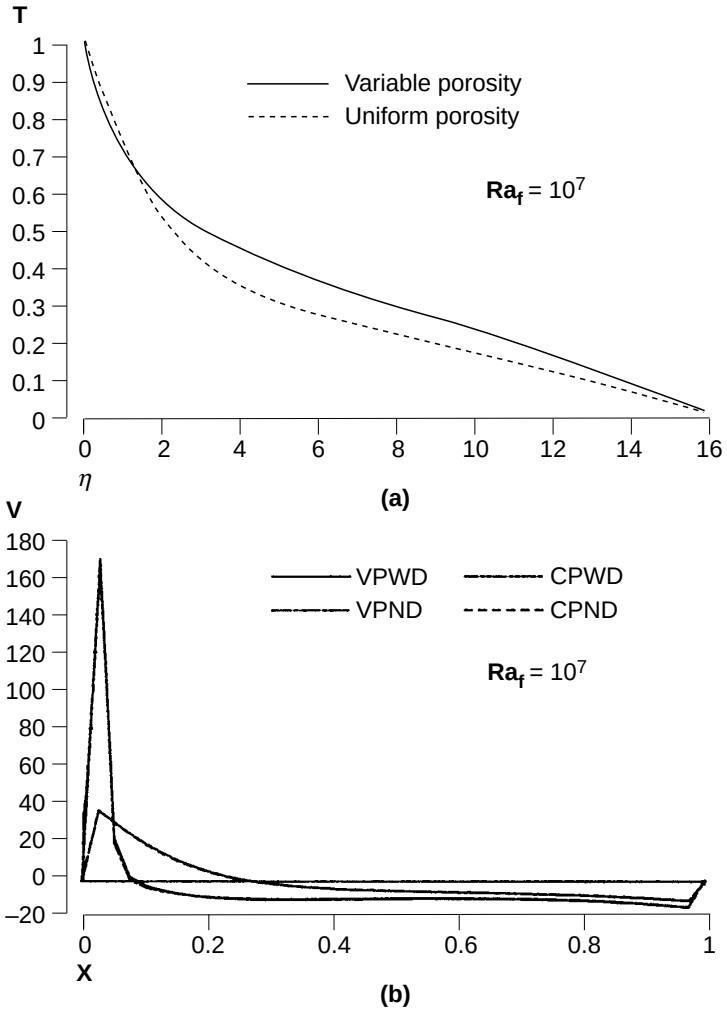

Figure 11. Effect of variable porosity on temperature and velocity distributions at $A = 1$, $\Gamma = 0.05$, $\theta = 0°$, and $\lambda = 0.6$; (a) temperature distribution; (b) velocity distribution

$\lambda = 0.6$, and $A = 1$ is presented in Figure 12. It can be concluded from this figure that thermal dispersion effect increases the heat transfer rate and its effect increases with increase in the dimensionless particle diameter Γ.

Figure 13 shows the effect of thermal dispersion on the Nusselt number as a function of the Rayleigh number at different dimensionless particle diameters for a uniform porosity medium heated from below. To compare the results with those from the BFD and the Darcy models, the numerical results obtained using three theoretical models are presented in this figure, where CPWD denotes results based on uniform porosity with dispersion effect, CPND denotes results based on uniform porosity without dispersion effect, and DLND denotes results based on Darcy's law without dispersion effect. It is shown that the results

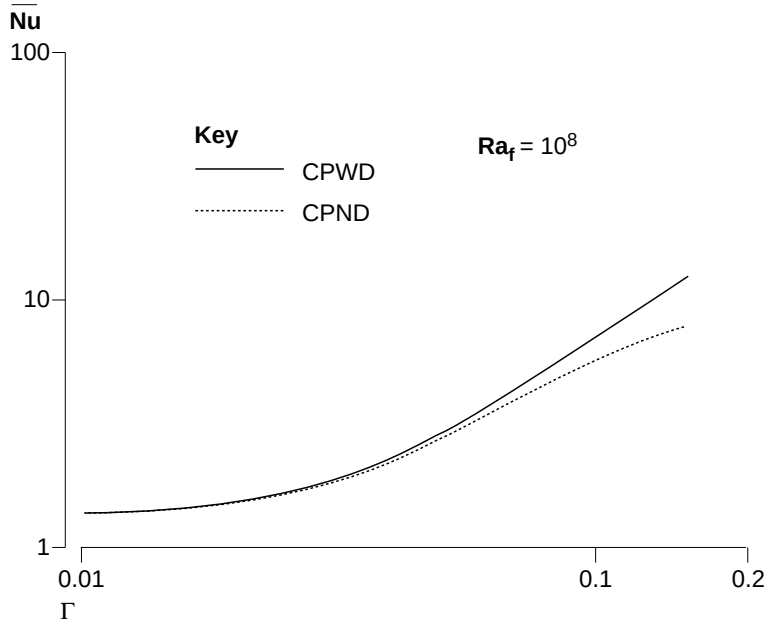

Figure 12.
Effect of thermal dispersion on mean Nusselt number (A = 1, θ = 90°)

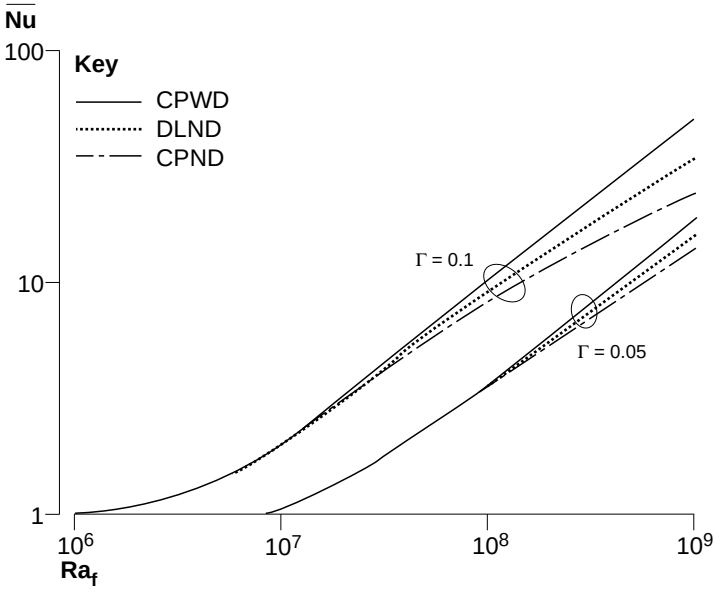

Figure 13.
Mean Nusselt number as a function of fluid Rayleigh number for a uniform porosity medium (A = 1, θ = 90°, and λ = 0.6)

based on the Darcy model lie between those based on the BFD model with and without thermal dispersion for a uniform porosity medium. The results show that the non-Darcian effects considered in the momentum equation, such as the inertia, viscosity and acceleration terms, reduce the heat transfer rate. Like the

variable porosity effect, the thermal dispersion effect tends to increase the temperature gradient adjacent to the wall and consequently to enhance the surface heat flux.

Effect of acceleration term

Figure 14 shows a comparison of computed Nusselt numbers (with and without the acceleration term) with the numerical results by Davis *et al.* (1988) and the experimental data obtained by Seki (1978) . It is shown that the acceleration term decreases the heat transfer rate slightly. The present results without the acceleration term are shown to be lower than those computed by Davis *et al.* (1988), who did not take the acceleration and thermal dispersion terms into consideration. This disparity can only be attributed to the differences in numerical methods and the grid size used.

Comparisons with experimental results

Table II compares the experimental data of Inaba *et al.* (1988) for the average Nusselt number with the present numerical solutions obtained using four

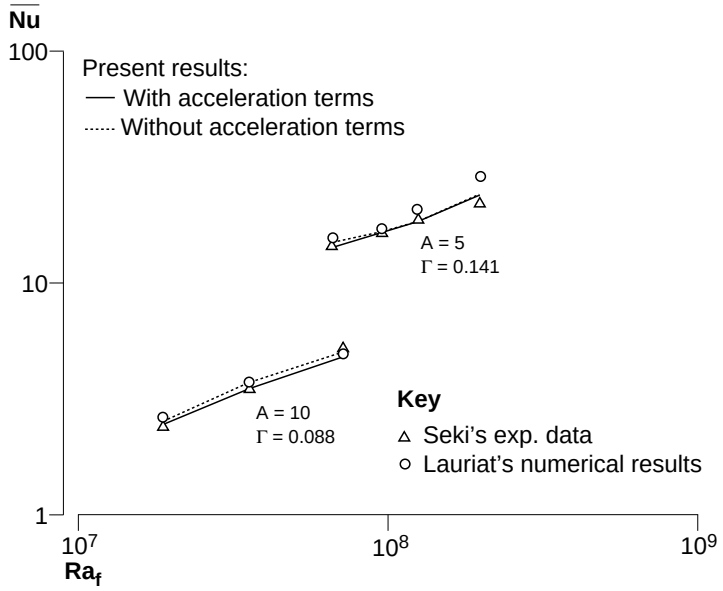

Figure 14. Comparison of calculated and measured Nusselt numbers for a square porous cavity heated from the side

Porous media	Γ	*A*	Ra_m	*θ*	Inaba *et al.* (1988)	Present results VPWD	VPND	CPWD	CPND
Water/glass	0.153	5	121	0°	3.64	3.124	3.014	2.441	2.287
Water/glass	0.153	5	1,260	0°	9.71	9.132	8.724	7.643	7.321

Table II. Comparison of Nusselt numbers from present results and previously published experimental data

theoretical models for natural convection in rectangular cavities filled with glass spheres saturated with water at $A = 5$, $\theta = 0°$, and $\Gamma = 0.153$. Ra_m in this Table denotes the Darcy-Rayleigh number which is defined as $Ra_m = g\beta_f KL_2 (T_h^* - T_c^*)/\alpha_e \upsilon_f$. The symbol VPWD represents results based on variable porosity with dispersion effect, and VPND represents those of variable porosity without dispersion effect. It is shown that the effect of thermal dispersion increases the heat transfer rate for both the uniform porosity and variable porosity models. The results based on the variable porosity model with thermal dispersion taken into consideration have the best agreement with experimental data. Figure 14 shows that the computed results agree with the experimental data obtained by Seki (1978).

Concluding remarks

Various effects on natural convection in an inclined porous cavity are investigated numerically. Some conclusions can be drawn from the present study:

(1) The Prandtl number effect is small for Pr >1; however, its effect increases as the Prandtl number decreases below one.

(2) The location of peak velocity is affected by the particle diameter.

(3) Both variable porosity and thermal dispersion effects increase the temperature gradient adjacent to the wall, resulting in the enhancement of surface heat flux. These effects become important when the dimensionless particle diameter is increased and can be neglected if conduction is dominant.

(4) The predicted Nusselt numbers based on the BFD model which takes into account wall effects on porosity, permeability, stagnant thermal conductivity and thermal dispersive conductivity have the best agreement with experimental data.

References

Beckermann, C., Viskanta, R. and Ramadhyani, S. (1986), "A numerical study of non-Darcian natural convection in a vertical enclosure filled with a porous medium", *Num. Heat Transfer,* Vol. 10, pp. 557-70.

Chan, B.K.C., Ivey, C.M. and Barry, J.M. (1970), "Natural convection in enclosed porous media with rectangular boundaries", *J. Heat Transfer*, Vol. 92, pp. 21-7.

Chandrasekhara, B.C. and Vortmeyer, D. (1979), "Flow model for velocity distribution in fixed beds under isothermal conditions", *Warme-und-Stoffubertrangung,* Vol. 12, pp. 105-11.

Cheng, P. (1978), "Heat transfer in geothermal systems", *Advances in Heat Transfer*, Vol. 14, pp. 1-105.

Cheng, P. (1981), "Thermal dispersion effects in non-Darcian convective flows in a saturated porous medium", *Letters in Heat Mass Transfer*, Vol.8, 267-70.

Cheng, P. (1986), "Heat conduction in packed bed with wall effects", *Int. Comm. Heat Mass Transfer*, Vol. 13, pp. 11-21.

Cheng, P. and Hsu, C.T. (1986a), "Application of Van Driest's mixing length theory to forced convection in porous medium", *Int. Comm. Heat Mass Transfer*, Vol. 13, pp. 613-25.

Cheng, P. and Hsu, C.T. (1986b), "Fully developed forced convective flow through an annular packed-sphere bed with wall effects", *Int. J. Heat Mass Transfer*, Vol. 29, pp. 1843-53.

Cheng, P. and Zhang, T.M. (1986), "Mixed convection in the thermal plume above a horizontal line source of heat in a porous medium of infinite extent", *Proceedings of the 8th International Heat Transfer Conference,* Vol. 5, pp. 2671-5.

Davis, E., Lauriat, G. and Cheng, P. (1988), "A numerical solution of variable porosity effects on natural convection in a packed-sphere cavity", *Proceedings of 25th ASME National Heat Transfer Conference*, Vol. 1, pp. 605-12.

Fand, R.M. and Phan, R.T. (1987), "Combined forced and natural convection heat transfer from a horizontal cylinder embedded in a porous medium", *Int. J. Heat Mass Transfer*, Vol. 30, pp. 1351-8.

Georgiadis, J.G. and Catton, I. (1988), "Dispersion in cellular thermal convection in porous layers", *Int. J. Heat Mass Transfer*, Vol. 31, pp. 1081-91.

Hong, J.T. and Tien, C.L. (1987a), "Analysis of thermal dispersion effect on vertical plate natural convection in porous media", *Int. J. Heat Mass Transfer*, Vol. 30, pp. 143-50.

Hong, J.T., Yamada, Y. and Tien, C.L. (1987b), "Effects of non-Darcian and nonuniform porosity on vertical plate natural convection in porous media", *J. Heat Transfer*, Vol. 109, pp. 356-62.

Hsiao, S.W., Cheng, P. and Chen, C.K. (1992), "Nonuniform porosity and thermal dispersion effects on natural convection about a heated horizontal cylinder in an enclosed porous medium", *Int. J. Heat Mass Transfer*, Vol. 35, pp. 3407-18.

Hsu, C.T. and Cheng, P. (1988), "Closure schemes of the macroscopic energy equation for convective heat transfer in porous media", *Int. Comm. Heat Mass Transfer*, Vol. 15, pp. 689-95.

Inaba, H., Sugawara, M. and Blumenberg, J. (1988), "Natural convection heat transfer in an inclined porous layer", *Int. J. Heat Mass Transfer*, Vol. 31, pp. 1365-74.

Jonsson, T. and Catton, I. (1987), "Prandtl number effect on Benard convection in porous media", *J. Heat Transfer*, Vol. 109, pp. 371-7.

Lauriat, G. and Prasad, V (1986), "Natural convection in a vertical porous cavity: a numerical study for Brinkman-extended Darcy formulation", in Prasad, V. and Hussain, N.A. (Eds), *Natural Convection in Porous Media*, ASME, New York, NY.

Poulikakos, D. (1985), "A departure from the Darcy model in boundary layer natural convection in a vertical porous layer with uniform heat flux from the side", *J. Heat Transfer*, Vol. 107, pp. 716-20.

Poulikakos, D. and Renken, K. (1987), "Analysis of forced convection in a duct filled with porous media", *J. Heat Transfer*, Vol. 109, pp. 880-8.

Prasad, V., Kulacki, F. A. and Keyhani, M. (1985), "Natural convection in porous media", *J. Fluid Mechanics*, Vol. 150, pp. 89-119.

Seki, N., Fukusako, S. and Inaba, H. (1978), "Heat transfer in a confined rectangular cavity packed with porous media", *Int. J. Heat Mass Transfer*, Vol. 21, pp. 985-9.

Tong, T.W. and Subramanian, E. (1985), "A boundary layer analysis for natural convection in vertical porous enclosures – use of the Brinkman-extended Darcy model", *Int. J. Heat Mass Transfer*, Vol. 28, pp. 563-71.

Vafai, K. (1984), "Convection flow and heat transfer in variable porosity media", *J. Fluid Mechanics*, Vol. 147, pp. 233-59.

Weber, J.E. (1975), "The boundary-layer region for convection in a vertical porous layer", *Int. J. Heat Mass Transfer*, Vol. 18, pp. 569-73.

Zehner, P. and Schluender, E.U. (1970), "Waermeleitfahigkeit Von Schuettungen bei massigen temperaturen", *Chem. Ingr. Tech*., Vol. 42, pp. 933-41.